Applied Microbiology and Biotechnology (2022) 106:5035–5049
https://doi.org/10.1007/s00253-022-12061-3

BIOTECHNOLOGICALLY RELEVANT ENZYMES AND PROTEINS

Insights into the xylan degradation system of *Cellulomonas* sp. B6: biochemical characterization of r*Cs*Xyn10A and r*Cs*Abf62A

Mercedes María Garrido[1,2] · Florencia Elizabeth Piccinni[1,2] · Malena Landoni[3] · María Jesús Peña[4] · Juliana Topalian[1] · Alicia Couto[3] · Sonia Alejandra Wirth[2] · Breeanna Rae Urbanowicz[5] · Eleonora Campos[1]

Received: 28 April 2022 / Revised: 21 June 2022 / Accepted: 26 June 2022 / Published online: 8 July 2022

Abstract

Valorization of the hemicellulose fraction of plant biomass is crucial for the sustainability of lignocellulosic biorefineries. The *Cellulomonas* genus comprises Gram-positive *Actinobacteria* that degrade cellulose and other polysaccharides by secreting a complex array of enzymes. In this work, we studied the specificity and synergy of two enzymes, *Cs*Xyn10A and *Cs*Abf62A, which were identified as highly abundant in the extracellular proteome of *Cellulomonas* sp. B6 when grown on wheat bran. To explore their potential for bioprocessing, the recombinant enzymes were expressed and their activities were thoroughly characterized. r*Cs*Xyn10A is a GH10 endo-xylanase (EC 3.2.1.8), active across a broad pH range (5 to 9), at temperatures up to 55 °C. r*Cs*Abf62A is an α-L-arabinofuranosidase (ABF) (EC 3.2.1.55) that specifically removes α-1,2 and α-1,3-L-arabinosyl substituents from arabino-xylo-oligosaccharides (AXOS), xylan, and arabinan backbones, but it cannot act on double-substituted residues. It also has activity on *p*NPA. No differences were observed regarding activity when *Cs*Abf62A was expressed with its appended CBM13 module or only the catalytic domain. The amount of xylobiose released from either wheat arabinoxylan or arabino-xylo-oligosaccharides increased significantly when r*Cs*Xyn10A was supplemented with r*Cs*Abf62A, indicating that the removal of arabinosyl residues by r*Cs*Abf62A improved r*Cs*Xyn10A accessibility to β-1,4-xylose linkages, but no synergism was observed in the deconstruction of wheat bran. These results contribute to designing tailor-made, substrate-specific, enzymatic cocktails for xylan valorization.

Key points

- *rCsAbf62A removes α-1,2 and α-1,3-L-arabinosyl substituents from arabino-xylo-oligosaccharides, xylan, and arabinan backbones.*
- *The appended CBM13 of rCsAbf62A did not affect the specific activity of the enzyme.*
- *Supplementation of rCsXyn10A with rCsAbf62A improves the degradation of AXOS and xylan.*

Keywords Hemicellulose · *Cellulomonas* · Xylanases · Arabinofuranosidases · GH10 · GH62

✉ Eleonora Campos
campos.eleonora@inta.gob.ar

[1] Instituto de Agrobiotecnología y Biología Molecular (IABIMO), CICVyA, Instituto Nacional de Tecnología Agropecuaria (INTA)- CONICET, Los Reseros y Nicolás Repetto S/N (1686), Hurlingham, Buenos Aires, Argentina

[2] Laboratorio de Agrobiotecnología, DFBMC- FCEN and Instituto de Biodiversidad y Biología Experimental y Aplicada (IBBEA) CONICET- Universidad de Buenos Aires (UBA), Pab. II, Ciudad Universitaria, C1428EG Buenos Aires, Argentina

[3] Centro de Investigación en Hidratos de Carbono (CIHIDECAR)- CONICET, Departamento de Química Orgánica, FCEN- Universidad de Buenos Aires (UBA), Pab. II, Ciudad Universitaria, C1428EG Buenos Aires, Argentina

[4] Complex Carbohydrate Research Center, University of Georgia, 315 Riverbend Road, Athens, GA, USA

[5] Department of Biochemistry and Molecular Biology, University of Georgia, 315 Riverbend Road, Athens, GA, USA

Introduction

Increasing environmental concerns and energy costs have resulted in a growing urgency to use plant biomass as a resource to produce fuels, chemicals, and bioproducts. However, the composition and biochemical properties of the secondary plant cell wall, which is the main component of plant biomass, confer resistance to deconstruction by microbes and enzymes, a trait known as biomass recalcitrance (Himmel 2008; Alonso et al. 2010; Zhao et al. 2012). The major constituents, cellulose, hemicellulose, and lignin, are arranged to form the plant cell wall, with a structure and relative composition that vary considerably between species, cell type, and developmental stage. Cellulose is tightly packed in microfibrils, which are aligned and bound together into fibril aggregates by a matrix of hemicellulose and lignin (Fahlen and Salmen 2003).

Hemicelluloses are the second most abundant polysaccharide on Earth after cellulose. These polysaccharides are complex and structurally diverse, and their deconstruction and/or valorization is crucial for the sustainability of lignocellulosic biorefineries (Qaseem et al. 2021). The predominant types of hemicelluloses in plant secondary cell walls are heteroxylans, including glucuronoxylans (GXs), arabinoxylans (AXs), and glucuronoarabinoxylans (GAXs), which have glucuronic acid and/or arabinose residues, decorating the β-1,4-xylose backbone (Rogowski et al. 2015). In particular, GAX and neutral AX are one of the main components of grasses and cereal crops (Pauly and Keegstra 2008; Saha 2003). AX has a high content of arabinose (33–45%) (Saha 2000), in single or double α-1,2 and/or α-1,3-L-arabinosyl substitutions of the xylan backbone (Perlin 1951).

In nature, enzymatic hydrolysis of xylans is performed by a diverse group of enzymes. Among them, endo-1,4-β-xylanases (XYNs) (EC 3.2.1.8), which hydrolyze the xylan backbone, can be found in nine different glycosyl hydrolase (GH) families: GH 5, 8, 10, 11, 30, 43, 51, 98, and 141, according to the carbohydrate-active enzymes (CAZy; www.cazy.org) database (Drula et al. 2022). These enzymes often act in concert with debranching enzymes that are able to remove substituents present on heteroxylans (Kormelink and Voragen 1993; Poutanen and Puls 1989; Bachmann and McCarthy 1991; Long et al. 2020). In this regard, α-L-arabinofuranosidases (ABFs) (EC 3.2.1.55, CAZy families GH 2, 3, 43, 51, 54 and 62), which remove α-1,2 and/or α-1,3-L-arabinosyl residues from the xylose backbone, are key for complete deconstruction of AX. The biochemical properties and activity profiles of all these enzymes need to be studied to evaluate their applications in the bioconversion of lignocellulosic biomass (Lagaert et al. 2014).

Significant advances in bioconversion of lignocellulosic biomass rely on identification of new microorganisms and enzymes that can utilize biomass from different plant sources and increase the efficacy of industrial processes. An encouraging approach is the exploration of microorganisms growing in aerobic environments where lignocellulose represents the main carbon-based nutrient source. Following this strategy, the strain *Cellulomonas* sp. B6 was obtained from a subtropical forest soil consortium (Campos et al. 2014). Genomic analysis of *Cellulomonas* sp. B6 revealed a wide set of genes encoding CAZymes with biotechnological potential (Piccinni et al. 2019). This novel isolate, related phylogenetically to *Cellulomonas flavigena*, was shown to secrete a repertoire of enzymes involved in xylan deconstruction when grown on wheat bran, wheat straw, and sugar cane straw. Enzymes identified in the extracellular proteome of *Cellulomonas* sp. B6 include six xylanases from families GH10, a xylanase GH11, and a debranching enzyme from family GH62 (Piccinni et al. 2019; Ontañon et al. 2021). The relative abundance of these enzymes varied depending on the culture carbon source substrate, suggesting differences in their biological role.

In this work, we cloned and biochemically characterized *Cs*Xyn10A and *Cs*Abf62A, which are among the most abundant proteins in the extracellular enzymatic extract of *Cellulomonas* sp. B6, when grown on wheat bran (Ontañon et al. 2021). We thoroughly characterized both enzymes and explored their possible synergism to understand their contribution to pentose utilization. We show that *Cs*Xyn10A is an endo-1,4-β-xylanase with no activity on cellulosic substrates (enzymes known as cellulase-free xylanases (Walia et al. 2017)) and *Cs*Abf62A is an α-L-arabinofuranosidase that selectively removes single α-1,2 and α-1,3-arabinosyl substituents, but not double substitutions, from xylan, arabinan, and xylo-oligosaccharides. To further study the role of these enzymes in biomass deconstruction, we determined their activity profiles and possible synergy. We also investigated the contribution of its native appended carbohydrate binding module CBM13 to the activity of *Cs*Abf62A.

Materials and methods

Bioinformatic analysis

The peptide sequences of *Cs*Xyn10A (GenBank KSW20567.1) and *Cs*Abf62A (GenBank KSW17752.1) were aligned using protein BLAST (BLASTP, NCBI database) (Altschul et al. 1990) against protein sequences from Protein Data Bank (pdb) (Berman et al. 2000) and reference proteins (refseq_protein) available in the NCBI database to identify putative catalytic residues. Protein parameter calculations and signal peptide predictions were performed using the ProtParam (Expasy; Swiss Institute of Bioinformatics)

and SignalP v5.0 (Almagro Armenteros et al. 2019) servers, respectively.The Swiss model (Waterhouse et al. 2018) was used to create three-dimensional models of the corresponding structures which were evaluated using GMQE and QMEAN values. These were 0.93 and 0.89, respectively, for *Cs*Abf62A (with pdb:4O8N as template), and 0.91 and 0.89, respectively, for *Cs*Xyn10A (with pdb:1E0V as template). Models were then rendered using VMD software (Humphrey et al. 1996).

Cloning and expression of rCsXyn10C

Total DNA from *Cellulomonas* sp. B6 was extracted using a Wizard® Genomic DNA Purification Kit (Promega, Madison, USA). The coding sequence for the mature *Cs*Xyn10A protein (1333 bp; amino acids 34–471) was amplified from 20 ng of bacterial genomic DNA, using *Taq* polymerase and primers gh10Emf (TTGGATCCGCCGCCGCCGGCAGCA CGCTCCAG) and gh10EMr (TTAAGCTTTTACGACGCC GAGCAGGTCAGCGTCGG). The amplified product was digested with *Bam*HI and *Hin*dIII restriction enzymes, gel purified (Wizard® SV Gel and PCR Clean-Up System, Promega, Madison, USA), and cloned into the protein expression vector pET28a using the same restriction sites (Novagen, Madison, USA). Correct integrity of the recombinant plasmid pET28a-His-*Cs*Xyn10A was corroborated by sequencing analysis (Macrogen, Seoul, Republic of Korea). The resulting pET28a-His-*Cs*Xyn10A construct encodes a fusion protein with a resulting N-terminal 6X histidine tag followed by amino acids 34–471 of *Cs*Xyn10A. Competent cells of *Escherichia coli* Rosetta (pLys) strain (Novagen, Madison, USA) were transformed for protein expression, which was induced in 250 mL cultures at $Abs_{600\,nm}$: 0.8 with 0.5 mM isopropyl β-D-1-thiogalactopyranoside (IPTG) for 16 h at 20 °C. Cells were centrifuged at 4000 g, 20 min, 4 °C, and the pellet was processed for recombinant protein purification.

Cloning and expression of rCsAbf62A and rCsAbf62A-cd

The complete gene coding for the mature *Cs*Abf62A protein (1416 bp; amino acids 23–493) and the sequence coding for the catalytic module alone (904 bp; amino acids 194–493) were amplified using the following primers: GH62Fw1 (AAAGGATCCGCGACCGTCGACACGAACGCGTAC)-GH62Rv (AAACTCGAGCTACCGCTGGAGCGTCAG CAGC) for r*Cs*Abf62A and GH62Fw2 (AAAGGATCCGTG CTCGCTGCCGAGCAGCTAC)-GH62Rv for r*Cs*Abf62A-cd. The amplified products were cloned into pET28a (Novagen, Madison, USA) as described above, but using *Bam*HI and *Xho*I restriction sites in these cases. The resulting pET28a-His-*Cs*Abf62A and pET28a-His-*Cs*Abf62A-cd constructs encode fusion proteins with a N-terminal 6X histidine tag followed by amino acids 23–493 and 194–493 of *Cs*Abf62A, respectively. *Escherichia coli* Arctic Express (DE3) competent cells (Agilent Technologies, Santa Clara, USA) were transformed with the plasmids and recombinant clones were induced with 1 mM IPTG for 24 h at 13 °C.

Recombinant protein purification and quantification

The QIA*expressionist* protocol (Qiagen; Germantown, USA) was used to test the solubility of the recombinant proteins and to purify them from the soluble intracellular fraction. Briefly, pellets from 250 mL induced cultures were resuspended in 25-mL lysis buffer (50 mM NaH_2PO_4, 300 mM NaCl, 10 mM imidazole pH 8.0), cells were lysed by sonication (2 cycles of 10 s ON- 10 s OFF pulses, for 2 min), and the soluble fraction was recovered by centrifugation (30 min, 10,000 g, 4 °C). Recombinant proteins were purified from the soluble fraction by immobilized metal affinity chromatography (IMAC) with Ni–NTA agarose resin (Qiagen; Germantown, USA), using 50 mM NaH_2PO_4, 300 mM NaCl, 250 mM imidazole pH 8.0 as elution buffer (QIA*expressionist*). Quantification of the purified proteins was determined by Bradford assay (Promega; Madison, USA) and with a nanodrop equipment (Thermo Fisher Scientific, Waltham, USA), using the corresponding molecular weight and extinction coefficient. The yields obtained were 65 mg/L of cell culture of purified r*Cs*Xyn10A and 30 mg/L of cell culture of purified r*Cs*Abf62A and r*Cs*Abf62A-cd.

Polyacrylamide gel electrophoresis and immunoblotting

Recombinant proteins in crude cell-free extracts were loaded into reducing 10% SDS-PAGE gels, run at 100 V, and transferred to 0.45-µm nitrocellulose membrane (Bio-Rad Laboratories Inc., Hercules, USA). The membrane was first incubated with 5% non-fat dried milk in Tris-buffered saline (TBS; 20 mM Tris–HCl, pH 7.5, 150 mM NaCl) O.N. at 4 °C, and then, Western blot was performed by probing the membrane with 0.1 µg/mL of polyclonal rabbit anti HIS antibody (Genescript, Piscataway, USA) for 1 h in agitation, washed three times with TBS buffer for 15 min, and then incubated with 1:15,000 dilution of alkaline phosphatase-linked goat anti rabbit antibody (Sigma Chemical Co., Saint Louis, USA), for 1 h in agitation. The membrane was washed with TBS buffer as previously specified, incubated with BREFA buffer (100 mM Tris–HCl, pH 9.5, 100 mM NaCl, 5 mM $MgCl_2$) for 10 min, and phosphatase activity was revealed by a chromogenic reaction using 5-bromo-4-chloro-3-indolyl phosphate (BCIP) and nitroblue tetrazolium (NBT) as substrates (Sigma Chemical Co., Saint Louis, USA).

Activity assays

Activity assays to test substrate specificity of r*Cs*Xyn10A were assayed using 0.5% polymeric substrates or 2 mM 4-nitrophenyl-β-D-xylopyranoside (*p*NPX). Reactions (0.1 mL) contained enzyme (final concentration 0.002–0.02 µM) or buffer and mixtures were incubated at 40–50 °C and pH 6.0 for 10–20 min. Reactions containing BX or CMC were stopped by boiling for 10 min, and the reaction products were analyzed by the quantification of reducing sugars by the 3,5-dinitrosalicylic acid (DNS) method (Miller et al. 1960). Reactions containing *p*NPX were stopped by the addition of 2% Na_2CO_3, and the released *p*-nitrophenol (*p*NP) was measured by reading the absorbance at 410 nm. Xylanase activity was additionally measured using 0.5% medium or low-viscosity wheat flour arabinoxylan (WAX-mv and WAX-lv, respectively) (Megazyme, Bray, Ireland), following the same procedure as for BX.

Typical reactions for assaying arabinofuranosidase activity of r*Cs*Abf62A and r*Cs*Abf62A-cd consisted of 2 mM *p*NP-α-L-arabinofuranose (Sigma Chemical Co., Saint Louis, USA) and 1 µM enzyme in sodium phosphate buffer pH 6.0. Reactions were allowed to proceed for 10 min and stopped with 2% Na_2CO_3 as described above. Further experiments were performed by incubating 0.5% (w/v) polymeric substrates and 0.1–1 µM enzyme at 30 °C for 5 to 60 min as indicated. Reaction products were quantified by the DNS method (Miller et al. 1960) (reducing sugars) and/or high-performance anion-exchange chromatography with pulsed amperometric detection (HPAEC-PAD) or visualized by thin-layer chromatography (TLC) or 1D ^{1}H nuclear magnetic resonance (NMR) spectroscopy.

For reactions performed with natural substrates, one unit (U) of xylanase or arabinofuranosidase activity was defined as the amount of enzyme that releases 1 µmol of xylose or arabinose per min at the reaction conditions. For commercial *p*-nitrophenol (*p*NP)-sugar substrates, activity was defined as the amount of enzyme that liberates 1 µmol *p*NP per min.

Activity assays using xylo-oligosaccharides (XOS), with degrees of polymerization (DP) 2 to 6 (X2-X6, Megazyme, Bray, Ireland), were performed by incubating 1.5 mg/mL substrate prepared in 50 mM citrate/phosphate buffer pH 6.5 with 0.01 µM of r*Cs*Xyn10A. Reactions were incubated at 45 °C for 0, 30, and 120 min, stopped by boiling, and cleared by centrifugation (10,000 g, 10 min). Activity assays using AXOS were performed in 50 µL reactions containing 50 mg/mL 3^3-α-L-arabinofuranosyl-xylotetraose (XA^3XX), 2^3-α-L-arabinofuranosyl-xylotriose (A^2XX) or 3^3-α-L-plus 2^3-α-L-arabinofuranosyl-xylotetraose mixture (XAXX-mix) (Megazyme, Bray, Ireland), and 0.5 µM of purified enzyme in 50 mM sodium phosphate buffer pH 6.0. Reactions were carried out at 30 °C and 300 rpm for 4–16 h. Reaction products were analyzed using HPAEC-PAD or TLC.

Simultaneous activity assays

Combined activity of the recombinant proteins was first evaluated by incubating 5 mg/mL AXOS (XA^3XX or XAXX mix) with 0.5 µM r*Cs*Xyn10A alone or with equal molar concentration of r*Cs*Abf62A or r*Cs*Abf62-cd. Reactions were incubated at 30 °C and pH 6.0 for 4 h and soluble reaction products were visualized by TLC. Similar enzymatic reactions were performed by incubating 0.5% WAX-lv with 0.1 µM r*Cs*Xyn10A and 0.6 µM r*Cs*Abf62A or r*Cs*Abf62A-cd at 30 °C for 5 h. The substrate was also incubated with each enzyme alone, in the same concentrations. Reactions were stopped by heating at 80 °C for 10 min and soluble reaction products were analyzed by HPAEC-PAD.

Alcohol insoluble residue (AIR) preparation from wheat bran

Wheat bran was first ground to reduce particle size and then suspended in 80% ethanol and homogenized. The material was filtered by 50-µm nylon mesh and washed thoroughly with 80% ethanol. The sample was resuspended in 1:1 chloroform/methanol, stirred for a minimum of 4 h, and re-filtered by 50-µm nylon mesh. AIR was obtained by drying the sample at room temperature after a thorough wash with acetone.

Reducing sugar analysis by the DNS method

Reducing sugars were analyzed by the DNS method (Miller et al. 1960). Briefly, 100 µL of the reaction products was mixed with 200 µL of DNS and boiled for 10 min, followed by a 10-min incubation on ice. Two hundred microliters of each mixture was transferred to a 96-well plate and absorbance was measured at 540 nm. Results were compared to a xylose standard curve (0–1 mg/mL) obtained under the same conditions. Control reactions without enzyme and/or substrate were included in the analysis.

Visualization of products by thin-layer chromatography (TLC)

TLC was performed using silica gel plates (Sigma-Aldrich, Saint Louis, USA) in a glass chamber. First the chamber was saturated overnight (O.N.) with 25 mL of butanol/acetic acid/water (2:1:1). The silica plate was seeded at the baseline with 2.5–10 µL of each reaction product and standards (0.25 mg/mL arabinose, xylose, xylobiose, or XOS with DP 3–6), and left to dry for 15 min at 30 °C. The seeded plate was incubated in the glass TLC chamber with the saturating solution as mobile phase, allowing two consecutive runs

(until mobile phase reached 1 cm below the upper end of the plate). Plates were then removed, dried, and revealed by spraying a solution of water/ethanol/sulfuric acid (20:70:3) with 1% orcinol, drying, and then heating slightly with a heat gun until visualization of sugars.

Product analysis by mass spectrometry

Reaction supernatant (10 µL) was incubated with 2 µL DOWEX-50 resin (Sigma-Aldrich, Saint Louis, USA) for 30 min at room temperature. Tubes were spun down and 1 µL of the supernatant was mixed with an equal volume of 10 mg/mL 2,5-dihydroxybenzoic acid (DHB) in methanol on a microSCOUT-MSP 96 target ground steel plate (Bruker, Billerica, USA). The spotted samples were then dried before being analyzed by mass spectrometry on a Microflex LT matrix-assisted laser desorption ionization time of flight (MALDI/TOF) instrument (Bruker, Billerica, USA).

Product analysis by high-performance anion-exchange chromatography with pulsed amperometric detection (HPAEC-PAD)

Arabinose, xylose, and xylobiose were analyzed by HPAEC-PAD in a CarboPac PA20 analytical column, 3 × 150 mm, and a CarboPac PA20 guard column, 3 × 30 mm, (Dionex, Thermo Fisher Scientific, Waltham, USA). After equilibration of the column with 50 mM NaOH for 5 min, sample aliquots of 20 µL were injected and separated at a flow rate of 0.4 mL/min at a constant temperature of 30 °C. The elution conditions were as follows: 0–5 min: from 0 to 40 mM NaAcO in 50 mM NaOH (curve 5); 5–11 min: from 40 to 150 mM NaAcO in 50 mM NaOH (curve 5), 11–15 min: 150 mM NaAcO in 50 mM NaOH. The detector temperature was set at 30 °C. Chromeleon software (Thermo Fisher, Waltham, USA) was used for processing and data acquisition. Integrated peak areas were compared to mono and oligosaccharide calibration standards (xylose, xylobiose, and arabinose) purchased from Megazyme (Bray, Ireland).

1D ^{1}H nuclear magnetic resonance (NMR) spectroscopy

Reactions (200 µL) containing 0.5% (w/v) WAX-mv (Megazyme, Bray, Ireland) and *Cs*Abf62A (1 µM), *Cs*Abf62A-cd (1 µM), or buffer were incubated at 30 °C and pH 6.0 for 24 h followed by a 10-min incubation at 80 °C to stop the reactions. Precipitation of the substrate was achieved by adding 400 µL of 70% ethanol and incubating at 4 °C 16 h. Samples were then centrifuged, and the pellets were resuspended in 200 µL of deterium oxide (99.9%; Cambridge Isotope Laboratories, Tewksbury, USA) and freeze-dried. The dried substrates were then resuspended again with 200 µL of deterium oxide and placed in a 3-mm NMR tube. 1D and 2D ^{1}H-NMR spectra were recorded with a Varian Inova NMR spectrometer (Varian, Inc., Agilent Technologies, Palo Alto, USA) operating at 600 MHz equipped with a 5-mm cold probe and with a sample temperature of 298 K. Chemical shifts are given in ppm relative to an internal dimethyl sulfoxide (DMSO) standard (δ^1H 2.721). The NMR spectra were processed using MNova software (Mestrelab Research S.L., Santiago de Compostela, Spain).

Determination of kinetic parameters

GraphPad 6.01 software (GraphPad Software Inc.) was employed to identify the best kinetics model for each recombinant enzyme and to calculate the kinetic parameters K_{cat}, K_M, and V_{max}.

Thermal shift assay

For thermal shift analysis, reactions (30 µL) containing 3 µL of a 1:10 dilution of SYPRO™ Orange protein gel stain (Sigma-Aldrich, Saint Louis, USA) in H_2O, and 5 µM purified enzyme in 50 mM sodium phosphate buffer pH 6.0, in the presence or absence of 10 mM $CaCl_2$, were incubated in a OneStep Plus qPCR System (Applied Biosystems, Waltham, USA). Melting curves were generated by measuring fluorescence intensity at a temperature gradient of 25–90 °C with 1 °C intervals. The melting temperature (T_m) of the proteins was determined for each condition tested.

Results

Recombinant expression of CsXyn10A and CsAbf62A

*Cs*Xyn10A and *Cs*Abf62A are both modular enzymes, with a GH catalytic domain (CD) and a carbohydrate binding module (CBM): GH10-CBM2 and CBM13-GH62. Homology-based comparisons and protein modeling allowed us to predict structure, catalytic residues, and potential calcium binding motifs (only present in *Cs*Abf62A) as well as to identify the sequence corresponding to the N-terminal signal peptide (they are both extracellular enzymes) and the catalytic (CD) and carbohydrate binding (CBM) modules (Supplementary Fig. S1a). These results supported the endo-1,4-β-xylanase (XYN; EC 3.2.1.8) prediction for *Cs*Xyn10A and α-L-arabinofuranosidase (ABF; EC 3.2.1.55) prediction for *Cs*Abf62A. To further characterize each protein, *Cs*Xyn10A (amino acids 34–471) and *Cs*Abf62A (amino acids 23–493) were expressed, lacking the native signal peptide, in *E. coli* as recombinant N-terminal His-tagged fusion proteins.

We also expressed only the CD of *Cs*Abf62A (*Cs*Abf62A-cd, amino acids 194–493) to evaluate the contribution of CBM13 to enzyme function. Recombinant (r) *Cs*Xyn10A, *Cs*Abf62A, and *Cs*Abf62A-cd were successfully produced and purified from the soluble fraction (Supplementary Fig. S1b).

Substrate specificity of rCsXyn10A

Hydrolytic activity of r*Cs*Xyn10A was evaluated on several substrates to characterize its specificity and mode of action. Specific activity was 444.3 ± 44.6 and 408.6 ± 69.8 UI/mg from beechwood xylan (BX) and low-viscosity wheat arabinoxylan (WAX-lv), respectively (by the DNS method, at 40 °C and pH 6.0). Analysis of the reaction products from BX hydrolysis by thin-layer chromatography (TLC) and matrix-assisted laser desorption/ionization time of flight (MALDI-TOF) mass spectrometry (MS) showed the enzyme released mainly X2 as well as XOS and xylose (X1) (Fig. 1a and c). No activity was detected on Avicel (crystalline cellulose), phosphoric acid swollen cellulose (PASC), carboxymethylcellulose (CMC), xylobiose (X2), and *p*-nitrophenyl xylopyranoside (*p*NPX) (Table 1), demonstrating that *Cs*Xyn10A is a cellulase-free endo-1,4-β-xylanase. Next, we evaluated the ability of r*Cs*Xyn10A to degrade linear XOS with degrees of polymerization (DPs) of 3 to 6 (X3-X6) and visualized the reaction products by TLC after 0, 30, and 120 min of incubation (Fig. 1b). In all cases, xylobiose (X2) was the main product, although xylotriose (X3) and xylose were also obtained, suggesting an endo-mechanism, with preference for internal sites. Based on the degradation pattern, we think that there is also a less favored exo-activity, releasing X1 from either the reducing or non-reducing end, which still remains to be determined.

Substrate specificity of rCsAbf62A and rCsAbf62A-cd

To date, the majority of characterized GH62 enzymes is type B arabinofuranosidases (ABFs), which have been described to act on polysaccharides as well as arabino-xylo-oligosaccharides (AXOS) and, in some cases, *p*-nitrophenyl-α-L-arabinofuranoside (*p*NPA) (while type A ABFs act only on

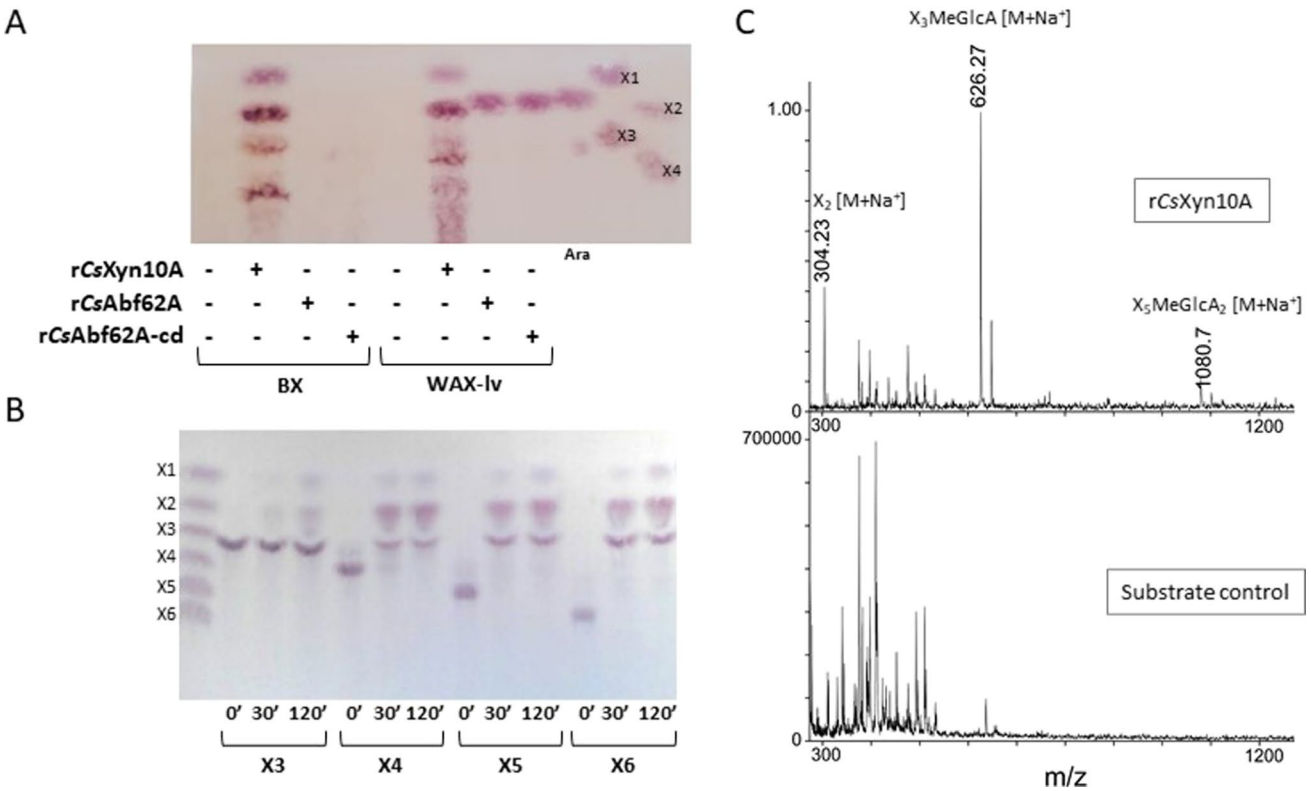

Fig. 1 Hydrolysis products of r*Cs*Xyn10A, r*Cs*Abf62A, and r*Cs*Abf62A-cd. **A** Thin-layer chromatography (TLC) of soluble reaction products of beechwood xylan (BX) and low-viscosity wheat arabinoxylan (WAX-lv) treated with the recombinant enzymes, as indicated (+). The lane with no enzymes corresponds to the substrate control. **B** TLC of soluble reaction products of r*Cs*Xyn10A on xylo-oligosaccharides (X3 to X6) with varying incubation times. TLC standards were loaded at 0.2 mg/mL: ARA (arabinose), X1 (xylose), X2 (xylobiose), X3 (xylotriose), X4 (xylotetraose), X5 (xylopentaose), and X6 (xylohexaose). **C** MALDI-TOF sprectra of reaction products of r*Cs*Xyn10A on BX. [a.u.]: arbitrary units. X_nMeGlcA [M + Na+]: sodium adduct of xylo-oligosaccharides with 4-*O*-methyl glucuronic acid with *n* degree of polymerization

Table 1 Substrate specificity analysis of r*Cs*Xyn10A, r*Cs*Abf62A, and r*Cs*Abf62A-cd

Substrate	Main linkages	Substitutions	r*Cs*Xyn10A	r*Cs*Abf62A/ r*Cs*Abf62A-cd
Wheat arabinoxylan (WAX) (low and medium viscosity)	Xyl β-1,4	Ara α-1,3/Ara α-1,2 (38%)	+ [a,b]	+ [a,b]
Beechwood xylan	Xyl β-1,4	GlcAOMe α-1,2 (13%)	+ [a,c]	- [a]
Poplar xylan	Xyl β-1,4	n.d	+ [a,c]	n.t
Wheat bran	n.d	n.d	+ [d]	+ [d]
XOS (DP 2–6)	Xyl β-1,4	-	+ [b]	n.t
XA^3XX	Xyl β-1,4	Ara α-1,3 (20%)	+ [b]	+ [b,d]
XAXX mix	Xyl β-1,4	Ara α-1,3/Ara α-1,2 (20%)	+ [b]	+ [b,d]
A^2XX	Xyl β-1,4	Ara α-1,2 (25%)	n.t	+ [b,d]
Sugar beet arabinan	Ara α-1,5	Ara α-1,3	n.t	+ [d]
Debranched arabinan	Ara α-1,5	-	n.t	- [c]
Larch arabinogalactan	Gal β-1,3	Ara α-1,6; Gal β-1,6Gal β-1,6; Ara α-1,4Gal β-1,6; Gal β-1,6Gal β-1,4	n.t	- [d]
Avicel PH-101	Glc β-1,4	-	- [a]	n.t
Phosphoric acid swollen cellulose	Glc β-1,4	-	- [a]	n.t
Carboxymethylcellulose	Glc β-1,4	40% CM	- [a]	n.t
*p*NP-α-L-arabinofuranoside	Ara α-1,4-*p*N	-	- [e]	+ [e]
*p*NP-β-D-xylopyranoside	Xyl β-1,4-*p*N	-	- [e]	- [e]
*p*NP-β-D-glucopyranoside	Glc β-1,4-*p*N	-	- [e]	- [e]

(+) presence or (−) absence of reaction products. Methods: a: DNS, b: TLC, c: MALDI-TOF, d: HPAEC-PAD, e: *p*NP assay; *n.t.*, not tested; *n.d.*, not determined

XOS, xylo-oligosaccharides; *XA3XX*, xylotetraose with 1,3-linked arabinose; *A2XX*, xylotriose with 1,2-linked arabinose (non-reducing end); *XAXX mix*, (50:50) XA3XX:XA2XX; *pNP*, *p*-nitrophenyl-; *CM*, carboxymethyl substituents; *Ara*, arabinose; *Gal*, galactose; *Glc*, glucose; *Xyl*, xylose; *GlcAOMe*, methylated glucuronic acid

AXOS and *p*NPA) (Wilkens et al. 2017). To characterize r*Cs*Abf62A, substrate specificity was determined using several polysaccharide substrates and monitored by measuring the release of arabinose substituents from WAX, wheat bran, and arabinan (Table 1). Specific activity was determined on WAX-lv for r*Cs*Abf62A (17.31 ± 1.03 IU/mg) and r*Cs*Abf62A-cd (23.56 ± 2.30 UI/mg) using the DNS method. Soluble reaction products were visualized by TLC, demonstrating that the enzyme hydrolyzed arabinose from WAX-lv (Fig. 1a). Release of arabinose was also confirmed for wheat bran, wheat xylan, and sugar beet arabinan by high-performance anion-exchange chromatography/pulsed amperometric detection (HPAEC-PAD). As for *p*NP substrates, r*Cs*Abf62A and r*Cs*Abf62A-cd were only able to hydrolyze *p*NPA, among the ones tested (*p*NP-β-D-xylopyranoside/-D-cellobioside/-β-D-lactobioside/-β-D-glucopyranoside).

To further determine the linkage-specificity of *Cs*Abf62A, we analyzed the activity on AXOS with different arabinose substitutions. Activity was tested using a XAXX mix (XA^3XX/XA^2XX) (xylotetraose with α-1,2 or α-1,3-linked arabinose substituents), XA^3XX (xylotetraose with α-1,3-linked arabinose), and A^2XX (xylotriose with α-1,2-linked arabinose). HPAEC-PAD analysis of the reaction products revealed r*Cs*Abf62A (and r*Cs*Abf62A-cd) was able to catalyze the complete hydrolysis of arabinose substituents on either the O-3 or O-2 positions of xylose, regardless of the position along the backbone (Supplementary Fig. S2).

Medium viscosity WAX (WAX-mv) is heavily substituted with arabinose (approximately 38%) and is known to have α-1,3 single and α-1,3 /α-1,2 double substitutions and little, if any, α-1,2 single substitutions (Pitkanen et al. 2009). To determine whether arabinose could be released from the single or doubly substituted xylose present in the polymer, ^{1}H NMR analysis was conducted after incubation of WAX-mv with r*Cs*Abf62A, r*Cs*Abf62A-cd, or buffer as control. Spectra obtained revealed the disappearance of the signal corresponding to 3-linked arabinofuranosyl residues attached to single substituted xylose, confirming complete degradation of this linkage, but not of the ones corresponding to arabinoses attached at O-3 and O-2 of the doubly substituted xylose (Fig. 2) (De Man et al. 2021). This could be related to the narrow active site pocket, capable of accommodating only one arabinose residue, in the cleft that accommodates the xylan backbone (dos Santos et al. 2018; Maehara et al. 2014).

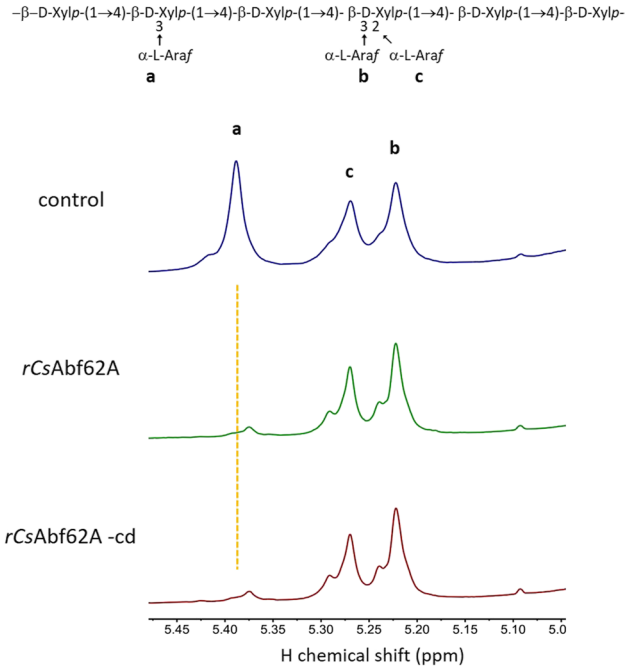

Fig. 2 1D ^{1}H NMR of r*Cs*Abf62A and r*Cs*Abf62A-cd wheat arabinoxylan reaction products. In the schematic, linkages within the polysaccharide (**a**–**c**) are labeled to correspond with peaks in the NMR spectra (**a**: α-1,3 linked Ara*f* in single substitutions; **b**: α-1,3 linked Ara*f* in double substitutions; **c**: α-1,2 linked Ara*f* in double substitutions). Spectra are vertically aligned and the yellow dotted line indicates the position of peak "a." The control spectrum is arabinoxylan that was incubated with protein buffer

When incubated with branched and debranched sugar beet arabinan, arabinose was released only from the former. Branched sugar beet arabinan consists of a α-1,5-linked arabinofuranose backbone to which α-1,3-linked (and possibly some α-1,2-linked) L-arabinofuranosyl residues are appended, whereas the debranched substrate has been enzymatically treated to remove all α-1,2 and α-1,3-L-arabinofuranosyl substituents from the backbone. Taken together, these data indicate that r*Cs*Abf62A is able to remove α-1,3 or α-1,2-arabinosyl substitutions from arabinan, but does not act upon the main α-1,5-linked arabinan backbone (Supplementary Fig. S3). The enzymes were tested alone or in combination with a commercial α-1,5-arabinanase (EC 3.2.1.99), and the DP of the oligosaccharide products (DP 2 to 5) did not change when r*Cs*Abf62A or r*Cs*Abf62A-cd were added, further supporting that this enzyme cannot act on α-1,5-arabinofuranosidic linkages in an endo or exo-manner (Supplementary Fig. S3). Moreover, no activity was observed on BX, which has α-1,2-linked 4-*O*-methyl glucuronic acid substituents (but no arabinose) or arabinogalactan from larch wood (ARGAL), which is appended with α-1,6-arabinosyl residues.

These results demonstrated unequivocally that *Cs*Abf62A is a type B GH62 enzyme with specific α-L-arabinofuranosidase activity that can only remove mono-substituted α-1,2 and α-1,3-linked arabinose residues but not α-1,2 α-1,3 double arabinose substitutions. Truncation of the CBM13 did not affect the activity or specificity for any of the substrates assayed.

Biochemical characterization of rCsXyn10A, rCsAbf62A, and rCsAbf62A-cd

Hydrolytic activity of the recombinant proteins was examined within a wide pH range (from 4.0 to 10.0), using BX for r*Cs*Xyn10A and *p*NPA for r*Cs*Abf62A and r*Cs*Abf62A-cd. The activity profile showed the highest activity at pH 6.0 for r*Cs*Xyn10A and 5.5 for r*Cs*Abf62A and r*Cs*Abf62A-cd (Fig. 3a). These conditions were used to determine the optimal reaction temperature of each enzyme and showed the maximum catalytic activity is at 50 °C for r*Cs*Xyn10A and 40 °C for r*Cs*Abf62A and r*Cs*Abf62A-cd (Fig. 3b).

Kinetic parameters of r*Cs*Xyn10A were calculated by monitoring the release of reducing sugars from increasing concentrations of BX by the DNS method (K_M 7.87 ± 1.03 mg/mL) and of r*Cs*Abf62A and r*Cs*Abf62A-cd by measuring *p*NP released from *p*NPA (K_M 2.47 ± 0.41 µM and 2.46 ± 0.60 µM, respectively). Data was fitted by nonlinear regression to the Michaelis–Menten model in all cases, suggesting a unique catalytic site with no secondary substrate binding sites (Fig. 3c).

Thermal stability was assayed by pre-incubation of the proteins at 30 to 50 °C for 4 to 24 h, prior to activity measurements (at optimal conditions for each enzyme). r*Cs*Xyn10A retained more than 80% activity after being pre-incubated at 40 °C for 24 h, indicating a high potential for application in bioprocesses at this temperature, while its activity significantly decreased after pre-incubation at 45 °C (retaining 30% activity after 24 h) and 50 °C (only 20% residual activity after 1 h) (Supplementary Fig. S4a). r*Cs*Abf62A and r*Cs*Abf62A-cd were active at lower temperatures than r*Cs*Xyn10A (Fig. 3) and also showed less thermal, with higher residual activity at 30 °C than at 40 °C (Supplementary Fig. S4c and e). The recombinant enzymes were active for at least 5 months stored at 4 °C, while they lost activity when stored at − 20 °C (without glycerol).

Melting curves of the recombinant proteins were analyzed by thermal shift assays, to further investigate their thermal stability. As there was a prediction of calcium binding sites for *Cs*Abf62A (Supplementary Fig. S1), the effect of calcium was also tested. The Tm, without the addition of $CaCl_2$, was 55° C, 40.9° C, and 41° C for r*Cs*Xyn10A, r*Cs*Abf62A, and r*Cs*Abf62A-cd, respectively. A positive shift of 3 °C was observed in the Tm (44.6° C) of both, r*Cs*Abf62A and r*Cs*Abf62A-cd, in the presence of 10 mM $CaCl_2$, suggesting that Ca^{2+} reduces the sensitivity of these proteins to thermal inactivation (Supplementary Fig. S4d and f). The shoulder

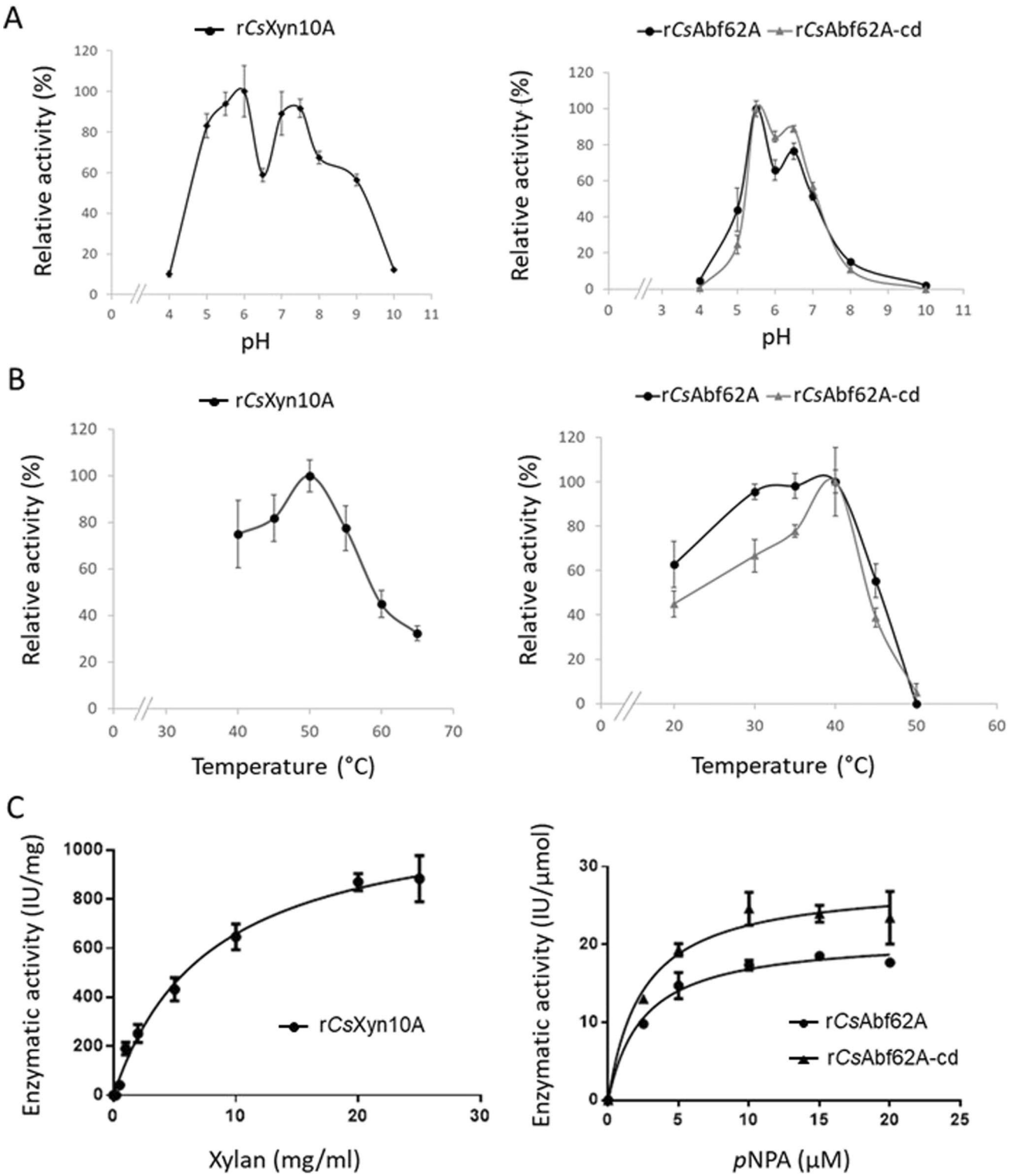

Fig. 3 Activity profile of r*Cs*Xyn10A, r*Cs*Abf62A, and r*Cs*Abf62A-cd. Optimal **A** pH condition, **B** temperature, and **C** substrate concentration, for the activity of r*Cs*Xyn10A (left) and r*Cs*Abf62A and r*Cs*Abf62A-cd (right). Optimal pH was determined at 50 °C for r*Cs*Xyn10A and 30 °C for r*Cs*Abf62A and r*Cs*Abf62A-cd. Optimal temperature was tested at pH 6.0 for all enzymes. The curves shown in **C** were obtained at 50 °C and pH 6.0 for r*Cs*Xyn10A and 30 °C and pH 5.5 for r*Cs*Abf62A and r*Cs*Abf62A-cd. Error bars indicate standard deviation of triplicates

present in the melting curve of r*Cs*Abf62A corresponds to the CBM13 module as it is not present in r*Cs*Abf62A-cd profile. As expected, no differences were observed for r*Cs*Xyn10A. These results are consistent with the predicted calcium binding sites in *Cs*Abf62A (absent in *Cs*Xyn10A). Also, hydrolytic activity of the proteins was analyzed in the presence of divalent ions. Activity of r*Cs*Xyn10A was not affected by the presence of Ca^{2+}, Cu^{2+}, Ni^{2+}, and Mg^{2+}, but it decreased significantly when incubated with Mn^{2+} and Co^{2+} (Supplementary Fig. S5). The increase in stability of r*Cs*Abf62A and r*Cs*Abf62A-cd in the presence of Ca^{2+} correlated with an improvement in activity, both at 30 and 40 °C (assayed on *p*NPA) (Supplementary Fig. S6).

Synergism in xylan degradation and substrate accessibility

Arabinose substitutions can hinder the hydrolytic activity of endo-1,4-β-xylanases and interfere with xylan depolymerization (Wong et al. 1988; Malgas and Pletschke 2019). Reaction products from WAX-lv hydrolysis using r*Cs*Xyn10A alone or in combination with r*Cs*Abf62A or r*Cs*Abf62A-cd were quantified by HPAEC-PAD and visualized by TLC. Our results showed that the release of X2 significantly increased when r*Cs*Abf62A or r*Cs*Abf62A-cd were added to r*Cs*Xyn10A (Table 2, Fig. 4a). Access to the substrate was also tested by investigating their combined ability to deconstruct arabino-xylo-oligosaccharides. Arabinose-substituted xylotriose (A^3XX, XA^3X, A^2XX, or XA^2X) and xylose (X1) were the main reaction products released from XA^3XX and XAXX-mix by r*Cs*Xyn10A alone, whereas xylobiose (X2) was also released when r*Cs*Abf62A, or r*Cs*Abf62A-cd, was added to the reaction (Fig. 4b). These results confirm that the enzymatic removal of arabinose substitutions increases r*Cs*Xyn10A accessibility to the substrate and enhances its xylanase activity.

Wheat bran digestion assays

*Cs*Xyn10A and *Cs*Abf62A were among the most abundant proteins in the extracellular enzymatic extract of *Cellulomonas* sp. B6 after growth in wheat bran (WB) as sole carbon source (Ontañon et al. 2021). WB is a composite that consists of layers of various tissues and the chemical fine structure of arabinoxylan varies in each layer. In addition to α-L-arabinofuranose substituents, some bran xylans contain complex sidechains and high content of ferulic acid esters residues (Saulnier et al. 2007). Composition analysis of the WB used for this study revealed a high arabinose content, with a ratio glucan:xylose:arabinose of 34:18:9.5 (Ontañon et al. 2021). We studied WB digestion by r*Cs*Xyn10A, r*Cs*Abf62A, and r*Cs*Abf62A-cd using as substrate the alcohol insoluble residue (AIR) of this biomass. The alcohol treatment of the biomass removes small sugars, proteins, nucleic acids, and lipids. When the enzymes were assayed individually, xylobiose was released from WB by r*Cs*Xyn10A and arabinose by r*Cs*Abf62A and r*Cs*Abf62A-cd (Fig. 5). Again, no effect of the CBM13 was observed for the release of arabinose from WB. When r*Cs*Xyn10A was assayed in combination with r*Cs*Abf62A (or r*Cs*Abf62A-cd) in the same proportion used for the WAX assay, the release of xylobiose remained unchanged, indicating that other factors, besides the single α-1,3- arabinose substitutions, may be acting as a bottleneck for deconstruction of this substrate. The presence of small phenolic compounds in WB, such as ferulic or *p*-coumaric acid, may also be interfering with the reaction (de Souza Moreira et al. 2013).

Discussions

Cellulomonas sp. B6 is a Gram-positive actinobacterium closely related to *Cellulomonas flavigena* that has proven to be a very valuable source for the production of carbohydrate-active enzymes (CAZymes). It secretes several CAZymes, mainly active on hemicelluloses, with variable relative abundance depending on the available carbon source. Among the extracellular proteins, a GH10-CBM2 (r*Cs*Xyn10A) and a GH62-CBM13 (*Cs*Abf62A) were identified in lignocellulosic biomass culture secretomes. These enzymes were highly abundant in wheat bran culture supernatant and less abundant in wheat straw and sugarcane straw supernatants (relative to all the secreted proteins), suggesting a preference for arabinoxylans (Piccinni et al. 2019; Ontañon et al.

Table 2 Concentration of xylobiose, xylose, and arabinose released from WAX-lv by r*Cs*Xyn10A alone or in combination with r*Cs*Abf62A or r*Cs*Abf62A-cd

Enzyme	X2 (mg/mL)	X1 (mg/mL)	Ara (mg/mL)
r*Cs*Xyn10A	0.14 ± 0.02 (4.26%)	0.05 ± 0.01 (1.44%)	n.d
r*Cs*Xyn10A + r*Cs*Abf62A	0.28 ± 0.04 (8.52%)*	0.05 ± 0.00 (1.44%)	0.17 ± 0.04 (7.99%)
r*Cs*Xyn10A + r*Cs*Abf62A-cd	0.27 ± 0.03 (8.22%)*	0.05 ± 0.01 (1.44%)	0.17 ± 0.03 (7.99%)

Quantification of reaction products by HPAEC-PAD and conversion rate (%) from the polysaccharide to xylobiose (X2), xylose (X1), and arabinose (Ara) is shown between parentheses. The values indicate means and standard deviations from triplicates. ANOVA and Tukey tests were performed to determine significant differences between means (*p-value < 0.05); *n.d.*, not detected

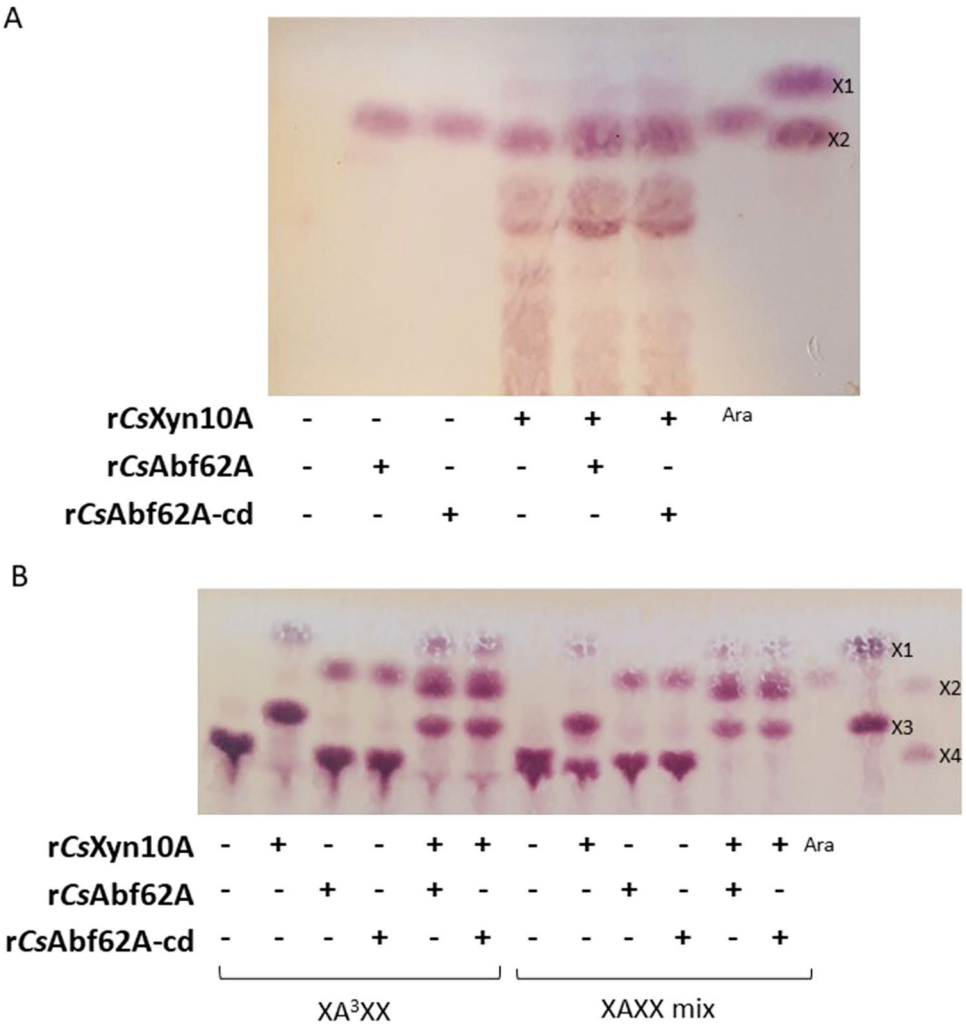

Fig. 4 Hydrolysis of WAX-lv and AXOS by r*Cs*Xyn10A and r*Cs*Abf62A or r*Cs*Abf62A-cd. Soluble reaction products generated by recombinant proteins after incubation with WAX-lv (**A**) or AXOS (**B**) were visualized by TLC. Reactions were carried out using enzymes individually or combinations of r*Cs*Xyn10A with r*Cs*Abf62A or r*Cs*Abf62A-cd, as indicated (+). XA^3XX: xylotetraose with 1,3-linked Ara*f*; XAXX mix: xylotetraose with 1,2- and 1,3-linked Ara*f*

2021). The most closely related homologues to these proteins in the *Cellulomonas* sp. reference strains were F4H4N7 (locus Celf_0088), from *Cellulomonas fimi* (83.1% identity, in 90% coverage, with r*Cs*Xyn10A), and D5UJU4 (locus Cfla_2848), from *C. flavigena* (75.4% identity, in 95% coverage, with CsAbf62A). These homologues have also been identified in studies of secretomes from common laboratory polysaccharide substrates (CMC and oat spelt xylan) cultures (Wakarchuk et al. 2016), which suggests they may play a core role in polysaccharides utilization.

In the present work, we demonstrated that r*Cs*Xyn10A has endo-1,4-β-xylanase activity (EC 3.2.1.8), with no additional glucanase or β-xylosidase activities, indicating it is an obligate xylanase. This is an important feature for eco-friendly pulp biobleaching applications, in which cellulase hydrolytic activity must be avoided to preserve cellulose fiber integrity (Walia et al. 2017). r*Cs*Xyn10A is active on different sources of xylan under moderate conditions (40 °C, pH 6), similarly to those reported for its *C. fimi* homologue (Khanna and Gauri 1993; Kane and French 2018).

As mentioned, *Cellulomonas* sp. B6 also secretes *Cs*Abf62A when cultured using wheat bran as the sole carbon source. According to the CAZy database, only 5 bacterial (and 19 eukaryotic) GH62 enzymes out of 637 known curated entries (April 2022) have been fully characterized biochemically, and there are several differences regarding modular structure and activity among them (Wilkens et al. 2017). r*Cs*Abf62A, similarly to most GH62s, is a type B α-L-arabinofuranosidase (ABF) (EC 3.2.1.55), as it was able to release arabinose decorations from AXOS as well as from the polymers, WAX and arabinan, and also had activity on *p*NPA, which is a variable feature for type B ABFs. The closest homologue to CsAbf62A characterized to date is an ABF from *Streptomyces lividans*, which also showed activity on xylan and arabinan decorations but very low activity towards *p*NPA (Vincent et al. 1997). r*Cs*Abf62A was able to release both α-1,2 and α-1,3-linked arabinose from single but not double-substituted xylose residues and was also able to remove single arabinose substituents from arabinan, an activity that has been reported

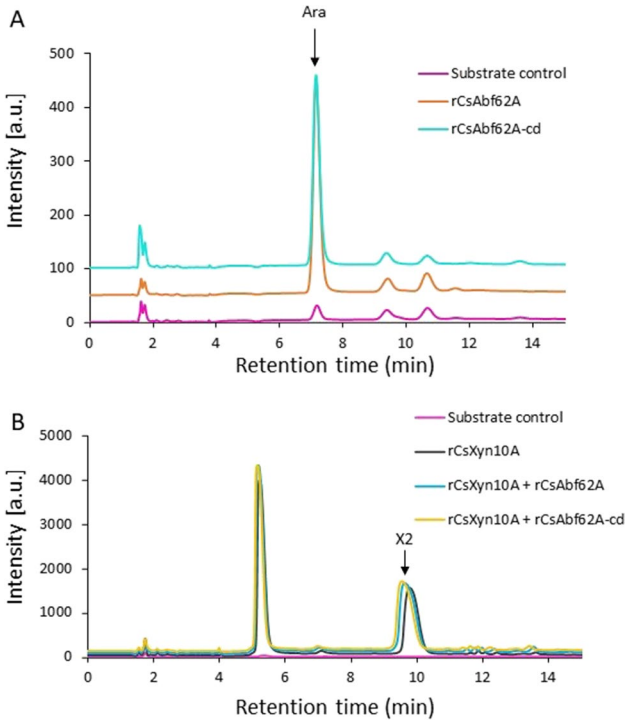

Fig. 5 Wheat bran (WB) digestion by **A** r*Cs*Abf62A or r*Cs*Abf62A-cd and **B** r*Cs*Xyn10A. HPAEC-PAD of soluble reaction products generated by r*Cs*Xyn10A (0.1 µM) and r*Cs*Abf62A or r*Cs*Abf62A-cd (0.6 µM) after incubation with WB (5% w/v) (pH 6, 30 °C, 48 h). Retention times were compared against commercial arabinose (Ara) and xylobiose (X2) standards

for some other GH62 enzymes, mostly with lower specific activity on arabinan than on arabinoxylan (Wilkens et al. 2017; Mroueh et al. 2019; Wang et al. 2014). Attempts have been made to classify GH62 in subfamilies (Siguier et al. 2014; Kaur et al. 2015), but most available information is related to sequence data and there is still not enough biochemical information to associate differences between the subfamilies with functional characteristics (Wilkens et al. 2017). Therefore, thorough biochemical characterization of GH62 enzymes is necessary to further characterize this family.

Structural analysis of GH62 ABFs showed that calcium ions bind to histidine in the conserved "SHG" motif stabilizing their tertiary conformation (Siguier et al. 2014; Tonozuka et al. 2017). The effect of this ion on the activity of GH62 proteins has had ambiguous results on other enzymes: Abf62C from *Scytadilium thermophilum* (Kaur et al. 2015), STX-IV from *Streptomyces thermoviolaceus* (Tsujibo et al. 2002), and *Cc*Abf62A from *Coprinopsis cinerea* (Tonozuka et al. 2017) were enhanced by Ca^{2+}, whereas activity of Abf62A from *S. thermophilum* was inhibited (Kaur et al. 2015). However, both catalytic activity and thermal stability of r*Cs*Abf62A were improved in the presence of $CaCl_2$. As biomass deconstruction requires multiple enzymes, the optimal calcium requirement would have to be established for each specific process, considering all enzymes involved.

According to Wilkens et al. (2017), 52% of GH62 members found in public databases (from 845 analyzed) have one or two xylan binding CBM13 domains. CBMs can be essential for efficient degradation of complex substrates by enabling enzyme substrate accessibility or by controlling the direction in which the enzymes move. However, no significant differences were observed in the substrate specificity or hydrolytic activity of the full-length enzyme when compared to the catalytic domain alone, in any of the conditions tested in this work. Further assays using more complex biomass substrates in high solid loading may help to unravel the contribution of the CBM13 module to the enzymatic degradation efficiency of *Cs*Abf62A.

Modification of xylans or specific xylan structures is of interest to the biomass-processing industry to allow full biomass degradation (Smith et al. 2017). Thus, much effort has been dedicated to the biochemical characterization of endo-1,4-β-xylanases, mainly from families GH10 and GH11. However, there is a growing interest in understanding the mechanistic action of debranching enzymes that act on hemicellulolytic polymers and their synergistic action with xylanases. Enzymes from GH62 are receiving increased attention for their valuable potential to be used in industrial processes, especially for cereal-derived feedstocks, and most of the characterizations of these enzymes have focused on crystallographic structures, phylogenetics, and specificity on model substrates (Phuengmaung et al. 2018). Here, we have demonstrated the potential of r*Cs*Xyn10A and r*Cs*Abf62A for biomass valorization efforts due to their ability to act on polymeric substrates and oligosaccharides. In particular, when harsh biomass pretreatment steps are replaced by milder hydrothermal pretreatment (HT), digestibility can be enhanced by coupling pretreatment to hemicellulose enzymatic hydrolysis. Also, the resulting liquid effluent is enriched in soluble xylan fragments and XOS, which could be then valorized in a C5-sugars utilization platform (Dutta et al. 2022). Synergic interactions were observed using AXOS and xylan, but not on wheat bran, indicating the importance of having a detailed knowledge of the substrate and the mechanism of action to adjust cocktail formulations in response to the composition and concentration of complex saccharide substrates in order to achieve full biomass conversion for enhanced utilization of C5 sugars in modern bio-refineries or functionalization of xylans for biomaterials and bioproducts. r*Cs*Xyn10A and r*Cs*Abf62A have shown activity in a wide range of pH and temperature conditions, supporting their potential to be evaluated for food and feed bioprocesses, in which xylanses and ABFs are required, such

as the production of prebiotic XOS or improving cereal based poultry feed (Alokika and Singh 2019; Poria et al. 2020).

Supplementary Information The online version contains supplementary material available at https://doi.org/10.1007/s00253-022-12061-3.

Acknowledgements M. L., A. C., S. A. W., and E. C. acknowledge the National Research Council of Argentina (CONICET) as Research Career Scientists. M. G. and J. T. hold PhD fellowships from CONICET. M. G. was recipient of a Visiting Scholar Fulbright Grant (2021) for a 3-month visit to BRU Lab at CCRC (Univ. of Georgia, USA). B. R. U. and M. J. P. are supported by the Center for Bioenergy Innovation (CBI), a U.S. Department of Energy Bioenergy Research Center supported by the Office of Biological, Environmental Research in the DOE Office of Science. B. R. U. also received support from the Chemical Sciences, Geosciences and Biosciences Division, Office of Basic Energy Sciences, U.S. Department of Energy Grant (DESC0015662) at the Complex Carbohydrate Research Center.

Author contribution M. M. G., E. C., M. J. P., and B. R. U. conceived and designed research and wrote the initial manuscript. M. M. G., F. E. P., M. L., M. J. P., J. T., and E. C. generated data and interpreted results. A. C. and S. A. W. discussed, analyzed, and interpreted data. All authors edited and commented on the manuscript. All authors reviewed and approved the final manuscript.

Funding This study was funded by Grants PICT2018-2983 and PICT2019-1474 (from the National Agency for Science and Technology Promotion from Argentina, ANPCyT) and Grant 20020130100476BA (from the University of Buenos Aires).

Data availability The complete sequences of *Cs*Xyn10A and *Cs*Abf62A are available at GenBank under the accession numbers KSW20567.1 and KSW17752.1 and at UniProtKB under A0A0V8SJU5 and A0A0V8SBR8, respectively. The datasets used and/or analyzed in the current study are available from the corresponding author on reasonable request.

Declarations

Ethical approval This article does not contain any studies with human participants or animals performed by any of the authors.

Conflict of interest The authors declare no competing interests.

References

AlmagroArmenteros JJ, Tsirigos KD, Sønderby CK, Petersen TN, Winther O, Brunak S, von Heijne G, Nielsen H (2019) SignalP 5.0 improves signal peptide predictions using deep neural networks. Nat Biotechnol 37(4):420–423. https://doi.org/10.1038/s41587-019-0036-z

Alokika, Singh B (2019) Production, characteristics, and biotechnological applications of microbial xylanases. Appl Microbiol Biotechnol 103:8763-8784. https://doi.org/10.1007/s00253-019-10108-6

Alonso DM, Bond JQ, Dumesic JA (2010) Catalytic conversion of biomass to biofuels. Green Chem 12:1493–1513. https://doi.org/10.1039/C004654J

Altschul SF, Gish W, Miller W, Myers EW, Lipman DJ (1990) Basic local alignment search tool. J Mol Biol 215:403–410. https://doi.org/10.1016/S0022-2836(05)80360-2

Bachmann SL, McCarthy AJ (1991) Purification and cooperative activity of enzymes constituting the xylan-degrading system of *Thermomonospora fusca*. Appl Environ Microbiol 57:2121–2130

Berman HM, Westbrook J, Feng Z, Gilliland G, Bhat TN, Weissig H, Shindyalov IN, Bourne PE (2000) The protein data bank. Nucleic Acids Res 28:235–242. https://doi.org/10.1093/nar/28.1.235

Campos E, Negro Alvarez MJ, Sabarís Di Lorenzo G, Gonzalez S, Rorig M, Talia P, Grasso D, Saéz F, Manzanares Secades P, Ballesteros Perdices M, Cataldi A (2014) Purification and characterization of a GH43 β-xylosidase from *Enterobacter* sp. identified and cloned from forest soil bacteria. Microbiol Res 169:213–220. https://doi.org/10.1016/j.micres.2013.06.004

De Man WL, Vaneeckhaute E, De Brier N, Wouters AGB, Martens JA, Breynaert E, Delcour JA (2021) 1H diffusion-ordered nuclear magnetic resonance spectroscopic analysis of water-extractable arabinoxylan in wheat (Triticum aestivum L.) flour. J Agric Food Chem 69(13):3912–3922. https://doi.org/10.1021/acs.jafc.1c00180

de Souza Moreira LR, de Carvalho CM, de Siqueira PH, Silva LP, Ricart CA, Martins PA, Queiroz RM, Filho EX (2013) Two β-xylanases from *Aspergillus terreus*: characterization and influence of phenolic compounds on xylanase activity. Fungal Genet Biol 60:46–52. https://doi.org/10.1016/j.fgb.2013.07.006

dos Santos CR, de Giuseppe PO, de Souza FHM, Zanphorlin LM, Domingues MN, Pirolla RAS, Honorato RV, Tonoli CCC, de Morais MAB, de Matos Martins VP, Fonseca LM, Büchli F, de Oliveira PSL, Gozzo FC, Murakami MT (2018) The mechanism by which a distinguishing arabinofuranosidase can cope with internal di-substitutions in arabinoxylans. Biotechnol Biofuels 11:223. https://doi.org/10.1186/s13068-018-1212-y

Drula E, Garron ML, Dogan S, Lombard V, Henrissat B, Terrapon N (2022) The carbohydrate-active enzyme database: functions and literature. Nucleic Acids Res 50:D571–D577. https://doi.org/10.1093/nar/gkab1045

Dutta N, Usman M, Luo G, Zhang S (2022) An insight into valorization of lignocellulosic biomass by optimization with the combination of hydrothermal (HT) and biological techniques: a review. Sustain Chem 3(1):35–55. https://doi.org/10.3390/suschem3010003

Fahlen J, Salmen L (2003) Cross-sectional structure of the secondary wall of wood fibers as affected by processing. J Mater Sci 38:119–126. https://doi.org/10.1023/A:1021174118468

Himmel (2008) Biomass recalcitrance; deconstructing the plant cell wall for bioenergy. Wiley-Blackwell, New Jersey

Humphrey W, Dalke A, Schulten K (1996) VMD - visual molecular dynamics. J Molec Graphics 14:33–38. https://doi.org/10.1016/0263-7855(96)00018-5

Kane SD, French CE (2018) Characterisation of novel biomass degradation enzymes from the genome of *Cellulomonas fimi*. Enzyme Microb Technol 113:9–17. https://doi.org/10.1016/j.enzmictec.2018.02.004

Kaur AP, Nocek BP, Xu X, Lowden MJ, Leyva JF, Stogios PJ, Cui H, Di Leo R, Powlowski J, Tsang A, Savchenko A (2015) Functional and structural diversity in GH62 α-L-arabinofuranosidases from the thermophilic fungus *Scytalidium thermophilum*. Microb Biotechnol 8(3):419–433. https://doi.org/10.1111/1751-7915.12168

Khanna S, Gauri (1993) Regulation, purification, and properties of xylanase from *Cellulomonas fimi*. Enzyme Microb Technol 15(11):990-995. https://doi.org/10.1016/0141-0229(93)90177-4

Kormelink FJM, Voragen AGJ (1993) Degradation of different [(glucurono)arabino]xylans by a combination of purified xylan-degrading enzymes. Appl Microbiol Biotechnol 38:688–695

Lagaert S, Pollet A, Courtin CM, Volckaert G (2014) β-Xylosidases and α-L-arabinofuranosidases: accessory enzymes for arabinoxylan

degradation. Biotechnol Adv 32(2):316–332. https://doi.org/10.1016/j.biotechadv.2013.11.005

Long L, Sun L, Lin Q, Ding S, St John FJ (2020) Characterization and functional analysis of two novel thermotolerant α-L-arabinofuranosidases belonging to glycoside hydrolase family 51 from *Thielavia terrestris* and family 62 from *Eupenicillium parvum*. Appl Microbiol Biotechnol 104(20):8719–8733. https://doi.org/10.1007/s00253-020-10867-7

Maehara T, Fujimoto Z, Ichinose H, Michikawa M, Harazono K, Kaneko S (2014) Crystal structure and characterization of the glycoside hydrolase family 62 α-L-arabinofuranosidase from *Streptomyces coelicolor*. J Biol Chem 289(11):7962–7972

Malgas S, Pletschke BI (2019) The effect of an oligosaccharide reducing-end xylanase, BhRex8A, on the synergistic degradation of xylan backbones by an optimised xylanolytic enzyme cocktail. Enzyme Microb Technol 122:74–81. https://doi.org/10.1016/j.enzmictec.2018.12.010

Miller GL, Blum R, Glennon WE, Burton AL (1960) Measurement of carboxymethylcellulase activity. Anal Biochem 2:127–132. https://doi.org/10.1016/0003-2697(60)90004-X

Mroueh M, Aruanno M, Borne R, de Philip P, Fierobe HP, Tardif C, Pages S (2019) The *xyl-doc* gene cluster of *Ruminiclostridium cellulolyticum* encodes GH43- and GH62-α-L-arabinofuranosidases with complementary modes of action. Biotechnol Biofuels 12:144. https://doi.org/10.1186/s13068-019-1483-y

NCBI Resource Coordinators (2016) Database resources of the National Center for Biotechnology Information. Nucleic Acids Res 44(D1):D7–D19. https://doi.org/10.1093/nar/gkv1290

Ontañon O, Bedo S, Ghio S, Garrido M, Topalian J, Jahola D, Fehér A, Valacco P, Campos E, Fehér C (2021) Optimization of xylanases production by two *Cellulomonas* strains and their use for biomass deconstruction. Appl Microbiol Biotechnol 105:4577–4588. https://doi.org/10.1007/s00253-021-11305-y

Pauly M, Keegstra K (2008) Cell-wall carbohydrates and their modification as a resource for biofuels. Plant J 54(4):559–568. https://doi.org/10.1111/j.1365-313X.2008.03463.x

Perlin AS (1951) Isolation and composition of the soluble pentosans of wheat flours. Cereal Chem 28:370–381

Phuengmaung P, Kunishige Y, Sukhumsirichart W, Sakamoto T (2018) Identification and characterization of GH62 bacterial α-L-arabinofuranosidase from thermotolerant *Streptomyces* sp. SWU10 that preferentially degrades branched L-arabinofuranoses in wheat arabinoxylan. Enzyme Microb Technol 112:22–28. https://doi.org/10.1016/j.enzmictec.2018.01.009

Piccinni FE, Ontañon OM, Ghio S, Sauka DH, Talia PM, Rivarola ML, Valacco MP, Campos E (2019) Secretome profile of Cellulomonas sp. B6 growing on lignocellulosic substrates. J Appl Microbiol 126(3):811–825. https://doi.org/10.1111/jam.14176

Pitkanen L, Virkki L, Tenkanen M, Tuomainen P (2009) Comprehensive multidetector HPSEC study on solution properties of cereal arabinoxylans in aqueous and DMSO solutions. Biomacromol 10(7):1962–1969. https://doi.org/10.1021/bm9003767

Poria V, Saini JK, Singh S, Nain L, Kuhad RC (2020) Arabinofuranosidases: characteristics, microbial production and potential in waste valorization and industrial applications. Bioresour Technol 304:123019. https://doi.org/10.1016/j.biortech.2020.123019

Poutanen K, Puls J (1989) The xylanolytic enzyme system of *Trichoderma reesei*. In: Lewis G, Paice M (eds) Plant cell wall polymers, biogenesis and biodegradation. American Chemical Society, Washington DC, pp 630–640

Qaseem MF, Shaheen H, Wu A (2021) Cell wall hemicellulose for sustainable industrial utilization. Renew Sust Energy Rev 144 (110996). https://doi.org/10.1016/j.rser.2021.110996

Rogowski A, Briggs J, Mortimer J, Tryfona T, Terrapon N, Lowe E, Baslé A, Morland C, Day A, Zheng H, Rogers T, Thompson P, Hawkins A, Yadav M, Henrissat B, Martens E, Dupree P, Gilbert H, Bolam D (2015) Glycan complexity dictates microbial resource allocation in the large intestine. Nat Commun 6:7481. https://doi.org/10.1038/ncomms8481

Saha BC (2000) α-L-arabinofuranosidases: biochemistry, molecular biology and application in biotechnology. Biotechnol Adv 18:403–423. https://doi.org/10.1016/s0734-9750(00)00044-6

Saha BC (2003) Hemicellulose bioconversion. J Ind Microbiol Biotechnol 30(5):279–291. https://doi.org/10.1007/s10295-003-0049-x

Saulnier L, Sado PE, Branlard G, Charmet G, Guillon F (2007) Wheat arabinoxylans: exploiting variation in amount and composition to develop enhanced varieties. J Cereal Sci 46:261–281. https://doi.org/10.1016/j.jcs.2007.06.014

Siguier B, Haon M, Nahoum V, Marcellin M, Burlet-Schiltz O, Coutinho PM, Henrissat B, Mourey L, O'Donohue MJ, Berrin JG, Tranier S, Dumon C (2014) First structural insights into α-L-arabinofuranosidases from the two GH62 glycoside hydrolase subfamilies. J Biol Chem 289(8):5261–5273. https://doi.org/10.1074/jbc.M113.528133

Smith PJ, Wang HT, York WS, Peña MJ, Urbanowicz BR (2017) Designer biomass for next-generation biorefineries: leveraging recent insights into xylan structure and biosynthesis. Biotechnol Biofuels 10:286. https://doi.org/10.1186/s13068-017-0973-z

Tonozuka T, Tanaka Y, Okuyama S, Miyazaki T, Nishikawa A, Yoshida M (2017) Structure of the catalytic domain of α-L-arabinofuranosidase from *Coprinopsis cinerea*, CcAbf62A, provides insights into structure-function relationships in glycoside hydrolase family 62. Appl Biochem Biotechnol 181:511–525. https://doi.org/10.1007/s12010-016-2227-0

Tsujibo H, Takada C, Wakamatsu Y, Kosaka M, Tsuji A, Miyamoto K, Inamori Y (2002) Cloning and expression of an α-L-arabinofuranosidase gene (*stxIV*) from *Streptomyces thermoviolaceus* OPC-520, and characterization of the enzyme. Biosci Biotechnol Biochem 66(2):434–438. https://doi.org/10.1271/bbb.66.434

Vincent P, Shareck F, Dupont C, Morosoli R, Kluepfel D (1997) New α-L-arabinofuranosidase produced by *Streptomyces lividans*: cloning and DNA sequence of the *abfB* gene and characterization of the enzyme. Biochem J 322:845–852. https://doi.org/10.1042/bj3220845

Wakarchuk WW, Brochu D, Foote S, Robotham A, Saxena H, Erak T, Kelly J (2016) Proteomic analysis of the secretome of *Cellulomonas fimi* ATCC 484 and *Cellulomonas flavigena* ATCC 482. PLoS ONE 11(3):e0151186. https://doi.org/10.1371/journal.pone.0151186

Walia A, Guleria S, Mehta P, Chauhan A, Parkash J (2017) Microbial xylanases and their industrial application in pulp and paper biobleaching: a review. 3 Biotech 7(1):11. https://doi.org/10.1007/s13205-016-0584-6

Wang W, Mai-Gisondi G, Stogios PJ, Kaur A, Xu X, Cui H, Turunen O, Savchenko A, Master ER (2014) Elucidation of the molecular basis for arabinoxylan-debranching activity of a thermostable family GH62 α-L-arabinofuranosidase from *Streptomyces thermoviolaceus*. Appl Environ Microbiol 80(17):5317–5329. https://doi.org/10.1128/AEM.00685-14

Waterhouse A, Bertoni M, Bienert S, Studer G, Tauriello G, Gumienny R, Heer FT, de Beer TAP, Rempfer C, Bordoli L, Lepore R, Schwede T (2018) SWISS-MODEL: homology modelling of protein structures and complexes. Nucleic Acids Res 46(1):296–303. https://doi.org/10.1093/nar/gky427

Wilkens C, Andersen S, Dumon C, Berrin JG, Svensson B (2017) GH62 arabinofuranosidases: structure, function and applications. Biotechnol Adv 35(6):792–804. https://doi.org/10.1016/j.biotechadv.2017.06.005

Wong K, Tan L, Saddler J (1988) Multiplicity of β-1,4-xylanase in microorganisms: functions and applications. Microbiol Rev 52(3):305–317. https://doi.org/10.1128/mr.52.3.305-317.1988

Zhao X, Zhang L, Liu D (2012) Biomass recalcitrance. Part I: the chemical compositions and physical structures affecting the enzymatic hydrolysis of lignocellulose. Biofuels Bioprod Bioref 6:465–482. https://doi.org/10.1002/bbb.1331